PHYSICAL REVIEW D **82,** 035016 (2010)

Scalar dark matter and standard model with four generations

Xiao-Gang He,[1,2] Shu-Yu Ho,[2] Jusak Tandean,[2] and Ho-Chin Tsai[2]

[1]*INPAC and Department of Physics, Shanghai Jiao Tong University, Shanghai*

[2]*Department of Physics, Center for Theoretical Sciences, and LeCosPA Center, National Taiwan University, Taipei*

(Received 30 April 2010; revised manuscript received 9 July 2010; published 25 August 2010)

We consider a scalar dark-matter (DM) model, the SM4+D, consisting of the standard model with four generations (SM4) and a real gauge-singlet scalar called darkon, D, as the WIMP DM candidate. We explore constraints on the darkon sector of the SM4+D from WIMP DM direct-search experiments, including CDMS-II and CoGeNT, and from the decay of a B meson into a kaon plus missing energy. We find that a sizable portion of the darkon parameter space is still compatible with the experimental data. Since the darkon-Higgs interaction may give rise to considerable enhancement of the Higgs invisible decay mode, the existence of the darkon could lead to the weakening or evasion of some of the restrictions on the Higgs mass in the presence of fourth-generation quarks. In addition, it can affect the flavor-changing decays of these new heavy quarks into a lighter quark and the Higgs boson, as the Higgs may subsequently decay invisibly. Therefore, we also study these flavor-changing neutral transitions involving the darkon, as well as the corresponding top-quark decay $t \to cDD$, some of which may be observable at the Tevatron or LHC and thus provide additional tests for the SM4+D.

DOI: 10.1103/PhysRevD.82.035016 PACS numbers: 95.35.+d, 12.60.−i, 14.65.Jk, 14.80.Bn

I. INTRODUCTION

The existence of dark matter (DM) in the Universe is now widely accepted. Various observations have established that DM makes up 23% of the total cosmic energy density [1]. Despite this evidence, however, the identity of the basic constituents of DM has so far remained a mystery. It is therefore important to explore different possible DM scenarios.

One of the popular candidates for DM is the weakly interacting massive particle (WIMP). To account for WIMP DM, the standard model (SM) of particle physics needs to be expanded. The simplest extension of the SM possessing a WIMP candidate is the SM+D, which combines the SM with a real SM-singlet scalar field D, dubbed darkon, to play the role of the DM. This darkon model and some variations of it have been much studied in the literature [2–12].

In this paper we explore a somewhat expanded darkon model we call SM4+D, which consists of the darkon and the SM extended by the inclusion of a fourth sequential generation of quarks and leptons. This SM with four generations (SM4) has received a lot of attention in recent years [13–24]. Among the reasons [13] that have been put forward for all this interest in the SM4 are that it is not ruled out by electroweak precision tests [14–16], offers possible resolutions for certain anomalies in flavor-changing processes [17–20], and might solve baryogenesis-related problems [21]. In view of the desirable features of the model, some of which however remain open questions, it is of interest also to consider integrating the darkon field into it, assuming that the new fermions are all unstable, in which case the SM4+D is the simplest WIMP DM model in the presence of the fourth generation. As we will elaborate later, the DM sector of the SM4+D can have important implications which are absent or suppressed in the SM+D with three generations (hereafter referred to as SM3+D). In particular, now that the LHC is operational, the extra fermions could give rise to processes involving the darkon, which are potentially observable after the LHC reaches full capacity in the near future.

In the next section we describe the main features of the SM4+D relevant to our study. Subsequently, after specifying the masses of the fourth-generation fermions, we extract the values of the darkon-Higgs coupling, to be used in later sections, and also compare them with their counterparts in the SM3+D. In Sec. III, we derive constraints on these darkon models from DM direct-search experiments at underground facilities. Recently there have been a number of such searches which can provide limits on some of the parameter space of the two models. We proceed in Sec. IV to discuss the complementarity of DM direct searches and Higgs studies at colliders in probing the darkon properties. The simultaneous existence of the darkon and fourth-generation fermions in the SM4+D can have a substantial impact on Higgs searches. Since ongoing and near-future DM direct-search experiments are not likely to be sensitive to darkon masses of a few GeV or less, other processes are needed to examine the models in this low-mass region. In Sec. V, we study such processes, focusing on the B-meson decay into a kaon and a pair of darkons, $B \to KDD$, which contributes to the B decay into K plus missing energy, $B \to K\not{E}$. There is currently experimental information on the latter decay which can be used to place restrictions on part of the darkon low-mass region. For the processes and quantities that we have mentioned up to this point, we find that the fourth-generation fermions can produce changes to the SM3+D

predictions by as much as a factor of a few, in either direction, which is not too dramatic. In order to explore more-striking differences between the two models, in Sec. VI we consider some implications of the new fermions for the darkon sector that are lacking or missing in the SM3+D. More specifically, we look at the Higgs-mediated flavor-changing top-quark decay $t \to cDD$, which is very suppressed in the SM3+D and can be greatly enhanced by contributions from new heavy quarks, and also deal with the corresponding decays of the fourth-generation quarks. These processes may be detectable at currently running or future colliders and, if observed, could offer additional means to probe darkon masses from zero up to hundreds of GeV. We give our conclusions in Sec. VII.

Before discussing the darkon sector of the SM4+D, we would like to summarize the relic-density requirements that any WIMP candidate has to meet. For a given interaction of the WIMP with SM4 particles, its annihilation rate into the latter and its relic density Ω_D can be calculated and are related to each other by the thermal dynamics of the Universe within the standard big-bang cosmology [25]. To a good approximation,

$$\Omega_D h^2 \simeq \frac{1.07 \times 10^9 x_f}{\sqrt{g_*} m_{\rm Pl} \langle \sigma_{\rm ann} v_{\rm rel} \rangle \ {\rm GeV}}, \qquad x_f \simeq \ln \frac{0.038 m_{\rm Pl} m_D \langle \sigma_{\rm ann} v_{\rm rel} \rangle}{\sqrt{g_* x_f}}, \tag{1}$$

where h is the Hubble constant in units of 100 km/(s · Mpc), $m_{\rm Pl} = 1.22 \times 10^{19}$ GeV is the Planck mass, m_D is the WIMP mass, $x_f = m_D/T_f$ with T_f being the freezing temperature, g_* is the number of relativistic degrees of freedom with masses less than T_f, and $\langle \sigma_{\rm ann} v_{\rm rel} \rangle$ is the thermally averaged product of the annihilation cross section of a pair of WIMPs into SM4 particles and the relative speed of the WIMP pair in their center-of-mass frame. Since Ω_D is known from observations, using the above relations one can extract the allowed range of $\sigma_{\rm ann}$ for each value of m_D.

II. BRIEF DESCRIPTION OF SM4+D

Being a WIMP DM candidate, the darkon D has to be stable against decaying into SM4 particles. This can be realized by assuming D to be a singlet under the SM4 gauge groups and introducing a discrete Z_2 symmetry into the model. Under the Z_2 transformation, $D \to -D$, while all SM4 fields are unchanged. Requiring, in addition, that the darkon interactions be renormalizable implies that D can interact with the SM4 fields only through its coupling to the Higgs-doublet field H. It follows that the general form of the darkon Lagrangian, besides the kinetic part $\frac{1}{2} \partial^\mu D \partial_\mu D$ and the SM4 terms, can be expressed as [2–4]

$$\mathcal{L}_D = -\frac{\lambda_D}{4} D^4 - \frac{m_0^2}{2} D^2 - \lambda D^2 H^\dagger H, \tag{2}$$

where λ_D, m_0, and λ are free parameters, and we have followed the notation of Ref. [10]. The parameters in the potential should be chosen such that D does not develop a vacuum expectation value, and the Z_2 symmetry is not broken, which will ensure that the darkon does not mix with the Higgs field, avoiding possible fast decays into other SM4 particles.

The Lagrangian in Eq. (2) can be rewritten to describe the interaction of the physical Higgs-boson h with the darkon as[1]

$$\mathcal{L}_D = -\frac{\lambda_D}{4} D^4 - \frac{(m_0^2 + \lambda v^2)}{2} D^2 - \frac{\lambda}{2} D^2 h^2 - \lambda v D^2 h, \tag{3}$$

where $v = 246$ GeV is the vacuum expectation value of H. The second term in $\mathcal{L}_D$ contains the darkon mass $m_D = (m_0^2 + \lambda v^2)^{1/2}$, and the last term, $-\lambda v D^2 h$, has a major role in the determination of the relic density of the darkon. Clearly this model has a small number of free parameters in its DM sector: the darkon mass m_D, the darkon-Higgs coupling λ, and the darkon self-interaction coupling λ_D, besides the physical-Higgs mass m_h. Our analysis will not involve λ_D.

For $m_D < m_h$, the relic density is found, at leading order, from the annihilation of a darkon pair into SM4 particles via Higgs exchange [2–4], namely, $DD \to h^* \to X$, where X indicates SM4 particles. Since the darkon is cold DM, its speed is nonrelativistic and, consequently, a darkon pair has an invariant mass $\sqrt{s} \simeq 2m_D$. With the SM4+D Lagrangian determined, the h-mediated annihilation cross section of a darkon pair into SM4 particles is then given by [4]

$$\sigma_{\rm ann} v_{\rm rel} = \frac{8\lambda^2 v^2}{(4m_D^2 - m_h^2)^2 + \Gamma_h^2 m_h^2} \frac{\sum_i \Gamma(\tilde{h} \to X_i)}{2m_D}, \tag{4}$$

where $v_{\rm rel} = 2|\boldsymbol{p}_D^{\rm cm}|/m_D$ is the relative speed of the DD pair in their center-of-mass frame, $\tilde{h}$ is a virtual Higgs boson having the same couplings to other states as the physical h, but with an invariant mass $\sqrt{s} = 2m_D$, and $\tilde{h} \to X_i$ is any kinematically possible decay mode of $\tilde{h}$. To determine $\Sigma_i \Gamma(\tilde{h} \to X_i)$, one first computes the h width and then sets m_h equal to $2m_D$. For $m_D \geq m_h$, darkon annihilation into a pair of Higgs bosons, $DD \to hh$, also contributes to $\sigma_{\rm ann}$, through s-, t-, and u channel as well as contact diagrams, with vertices arising from the last two terms of $\mathcal{L}_D$ in Eq. (3) and the Higgs self-interaction (see, e.g., Ref. [6]). This becomes one of the leading contributions to $\sigma_{\rm ann}$, along with $DD \to h^* \to WW, ZZ$, if $m_D \gg m_{W,Z,h}$ [3,4].

[1]Obviously, h here is not to be confused with the Hubble constant, also denoted by h, in the combination $\Omega_D h^2$.

Compared to the SM3+D case, one effect of the fourth generation of quarks and leptons in the SM4+D is to enlarge the Higgs total width, Γ_h, and also the total width $\Sigma_i \Gamma(\tilde{h} \to X_i)$ of the virtual Higgs, $\tilde{h}$. These new heavy fermions contribute to the total widths mainly via the decay modes into fermion-antifermion pairs if kinematically possible and, exclusively for the new quarks, the decay mode into a gluon pair induced by a quark loop. Needless to say, the changes caused by the presence of these fermions depend on their masses.

There are constraints on the masses of the fourth-generation fermions from currently available experimental data. The masses of the heavy charged-lepton ℓ' and heavy neutrino ν', both assumed to be unstable, have the lower bounds $m_{\ell'} > 100.8$ GeV and $m_{\nu'} > 90.3$ GeV, according to the Particle Data Group [1]. For the masses of the fourth-generation up- and down-type quarks, t' and b', respectively, the strongest limits are $m_{t'} > 311$ GeV and $m_{b'} > 338$ GeV from searches at the Tevatron [26]. The mass differences between the new quarks and between the new leptons turn out to be subject to empirical constraints as well. Electroweak precision data prefer $m_{t'} - m_{b'} \simeq [5 + \ln(m_h/115\ \text{GeV})] \times 10$ GeV and 30 GeV $\lesssim m_{\ell'} - m_{\nu'} \lesssim$ 60 GeV [15]. Thus, for numerical work in this paper we take for definiteness $m_{\ell'} = 200$ GeV, $m_{\nu'} = 150$ GeV, $m_{t'} = m_{b'} + 55$ GeV, and $m_{t'} = 500$ GeV, but we also sometimes make comparisons with the $m_{t'} = 400$ and 600 GeV cases. We remark that these $m_{t'}$ values fall within the ranges allowed by recent global fits for the SM4 [15–19], although $m_{t'} = 600$ GeV is slightly above the unitarity upper bound of ~550 GeV [13,27].

With these mass choices, we can find the Higgs total widths, which we subsequently apply in Eq. (4), combined with the $DD \to hh$ contribution if $m_D \geq m_h$, in order to extract the darkon-Higgs coupling λ for given values of m_D, m_h, and $\langle \sigma_{\text{ann}} v_{\text{rel}} \rangle$. The allowed range of $\langle \sigma_{\text{ann}} v_{\text{rel}} \rangle$ as a function of m_D can be inferred, with the aid of Eq. (1), from the data on the relic density. Its most recent value is $\Omega_D h^2 = 0.1123 \pm 0.0035$, determined by an analysis of the seven-year data from the Wilkinson Microwave Anisotropy Probe combined with other data [28]. From this number, one can derive the 90% C.L. range $0.1065 \leq \Omega_D h^2 \leq 0.1181$, which we adopt for our numerical study. We show in Fig. 1 the resulting ranges of λ, taken to be positive, corresponding to 3 GeV $\leq m_D \leq 1$ TeV for some specific values of the Higgs mass, which we choose to be $m_h = 115$, 200, and 300 GeV for illustration. We present results both in the SM3+D and in the SM4+D with $m_{t'} = 500$ GeV for comparison purposes. Since the SM4+D values of λ turn out to be roughly similar to the SM3+D ones in Fig. 1(a), to reveal their differences clearly, we plot in Fig. 1(b) the ratio of the former to the latter. The ratio curves in the SM4+D cases with $m_{t'} =$ 400 and 600 GeV are not very different from the one displayed.

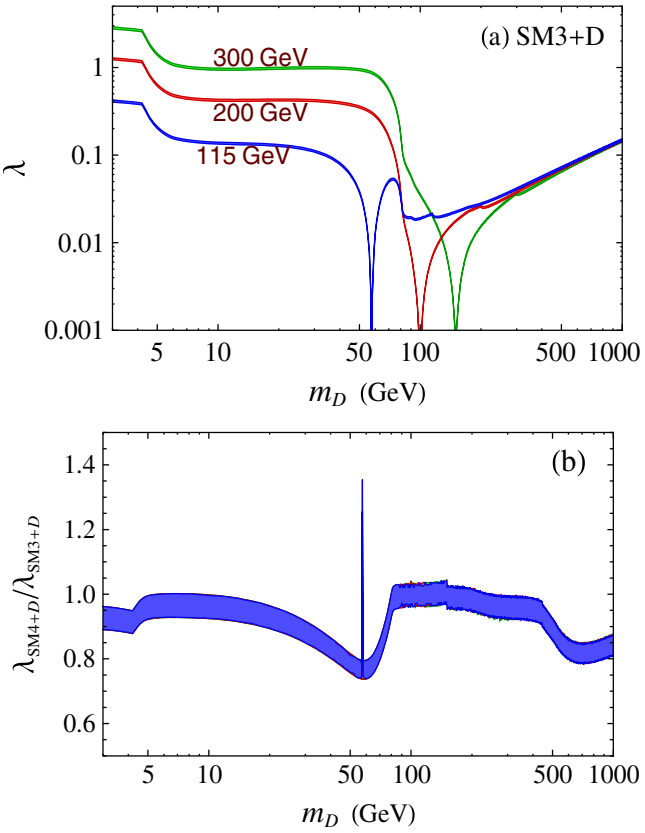

FIG. 1 (color online). (a) Darkon-Higgs coupling λ as a function of darkon mass m_D for Higgs-mass values $m_h = 115$, 200, 300 GeV in SM3+D. (b) Ratio of corresponding λ in SM4+D, with $m_{t'} = 500$ GeV, to λ in SM3+D. The band widths in all figures follow from the relic-density range which we have taken, $0.1065 \leq \Omega_D h^2 \leq 0.1181$.

There are several points worth pointing out in relation to what can be seen in Fig. 1. First, although only a relatively narrow range of the DM relic density is allowed, evidently it can be fairly easily reproduced in both the SM3+D and SM4+D. Second, λ is not small for the lower values of m_D, and this leads to a considerable branching ratio of the Higgs invisible decay mode in the two models, as we will discuss further later. Third, for 3 GeV $\leq m_D \lesssim 5$ GeV the size of λ can exceed unity and the $m_h = 300$ GeV curve approaches 3 at $m_D \sim 3$ GeV. This may seem to signal the breakdown of perturbativity in the low-m_D range, but an investigation into the perturbative unitarity of darkon-Higgs interactions at tree level [6] has come up with the limit $|\lambda| < 4\pi \simeq 12.6$. Furthermore, it has been suggested in Ref. [7] that, due to a lack of clear division between the perturbative and nonperturbative regions of the parameter space, a reasonable requirement is $|\lambda| < 2\sqrt{\pi}(m_h/100\ \text{GeV})^2$, which is roughly comparable to the preceding limit for the Higgs masses we have picked. Fourth, the steep decline of λ right after $m_D \sim 4.2$ GeV marks the sharp increase of $\Sigma_i \Gamma(\tilde{h} \to X_i)$ in Eq. (4) due to the opening of the $\tilde{h} \to b\bar{b}$ channel. This behavior of λ has

to do with the fact that $\langle\sigma_{\rm ann}v_{\rm rel}\rangle$ is roughly constant, of order 2×10^{-9} GeV^{-2} [1,10], for the m_D range of interest. Fifth, since $\sigma_{\rm ann}v_{\rm rel}$ varies little, each of the dips of the λ curves corresponds to the minimum of the denominator in Eq. (4) at the resonant point $m_D = m_h/2$. Sixth, although the λ values tend to become small as m_D enters the region between 50 and 200 GeV or so, they get large again, approximately linearly with m_D, as m_D grows sufficiently large. This follows from the fact $\sigma_{\rm ann}v_{\rm rel} \simeq \lambda^2/(4\pi m_D^2)$ for $m_D \gg m_{W,Z,h,t'}$ [3,4,10], while $\sigma_{\rm ann}v_{\rm rel}$ stays unchanged.

Lastly, the ratio curves in Fig. 1(b) for the three different m_h values nearly coincide at the majority of the m_D values considered. Evidently, the SM4+D numbers for λ are mostly lower than their SM3+D counterparts, the decrease being mainly less than 20%, but reaching ~25% in the neighborhood of $m_D \sim 60$ GeV, one of the exceptions being the spike belonging to the $m_h = 115$ GeV curve at the resonant point $m_D = 57.5$ GeV. The reason for the decrease is that the Higgs total width in the SM4 is, as mentioned earlier, enlarged relative to that in the SM3, which is also true for the total width of $\tilde{h}$ in Eq. (4), the enlargement ranging mainly from a few percent to ~40% and becoming as high as ~70% in the vicinity of $m_D \sim 60$ GeV. As for the spike at $m_D = 57.5$ GeV, we can understand its origin by first noting that Eq. (4) implies the relation $\lambda_{\rm SM4+D}/\lambda_{\rm SM3+D} = (\Gamma_h^{\rm SM4}/\Gamma_h^{\rm SM3})^{1/2}$ at the resonant point $m_D = m_h/2$. Then we find numerically that for $m_h = 115$ GeV this λ ratio is ~1.3 and the width of the spike is much less than 1 GeV, whereas for $m_h = 200$ and 300 GeV the ratios are both about 1.0, all of which can be viewed in Fig. 1(b). The sizable increase of $\Gamma_h^{\rm SM4}$ over $\Gamma_h^{\rm SM3}$ for $m_h = 115$ GeV arises from the much enhanced contribution of the $h \to gg$ mode to Γ_h caused by the 4th-generation quarks, but this increase is much reduced for $m_h = 200$ and 300 GeV in which cases Γ_h is highly dominated by the $h \to WW, ZZ$ modes [15]. In the next section, we encounter another quantity, the Higgs-nucleon effective coupling, which is also affected by the fourth-generation via the $h \to gg$ vertex.

III. CONSTRAINTS FROM DARK-MATTER DIRECT SEARCHES

A number of underground experiments have been and are being performed to detect DM directly by looking for the recoil energy of nuclei caused by the elastic scattering of a WIMP off a nucleon [29–34]. Although indirect DM searches have recently turned up some intriguing findings which may be interpreted as evidence for WIMPs [35], it is very difficult to establish a firm connection to DM due to the indirect nature of the observed events. Therefore, direct detection is crucial to determine the properties of DM.

In the SM4+D, as in the SM3+D, the WIMP-nucleon interaction occurs via the exchange of a Higgs boson between the darkon and the nucleon N in the t-channel process $DN \to DN$. Thus, to evaluate this elastic scattering requires knowing not only the darkon-Higgs coupling λ, but also the Higgs-nucleon coupling g_{NNh}, which parametrizes the Higgs-nucleon interaction described by $\mathcal{L}_{NNh} = -g_{NNh}\bar{N}Nh$. From this Lagrangian and $\mathcal{L}_D$ in Eq. (3), one can derive for $|t| \ll m_h^2$ the darkon-nucleon elastic cross section [2–4,8,9]

$$\sigma_{\rm el} \simeq \frac{\lambda^2 g_{NNh}^2 v^2 m_N^2}{\pi(m_D + m_N)^2 m_h^4}, \tag{5}$$

having used the approximation $(p_D + p_N)^2 \simeq (m_D + m_N)^2$.

It remains to determine the value of g_{NNh}, which is related to the underlying Higgs-quark interaction described by $\mathcal{L}_{qqh} = -\Sigma_q m_q \bar{q}qh/v$, where in the SM4 the sum runs over the eight quark flavors, $q = u, d, s, c, b, t, b', t'$. Since the energy transferred in the darkon-nucleon scattering is very small, of order tens of keV, one can employ a chiral-Lagrangian approach to estimate g_{NNh}. This has been done previously in the context of the SM3 [9,36,37]. In the SM4 case, we modify the derivation described in Ref. [9], incorporating the t' and b' contributions, to arrive at

$$g_{NN\mathcal{H}}^{\rm SM4} = \frac{m_N - \frac{17}{27}m_B}{v}, \tag{6}$$

where m_N is the nucleon mass and m_B denotes the lightest octet-baryon mass in the chiral limit, which can be related to the pion-nucleon sigma term, $\sigma_{\pi N}$, by $m_B \simeq -13.39\sigma_{\pi N} + 1.269$ GeV [9]. With $\sigma_{\pi N} = 45$ MeV [38], we obtain

$$g_{NNh}^{\rm SM4} = 2.11\times10^{-3}, \tag{7}$$

to be compared with the SM3 value $g_{NNh}^{\rm SM3} = 1.71\times10^{-3}$ [9]. We adopt these numbers in our numerical calculations below. We note, however, that $\sigma_{\pi N}$ is not well determined, with values ranging roughly from 35 MeV to 80 MeV having been quoted in the literature [37–39], which translate into $1.8\times10^{-3} \lesssim g_{NNh}^{\rm SM4} \lesssim 3.3\times10^{-3}$ and $1.3\times10^{-3} \lesssim g_{NNh}^{\rm SM3} \lesssim 3.2\times10^{-3}$.

With λ and g_{NNh} known, we can now predict the darkon-nucleon elastic cross-section $\sigma_{\rm el}$ as a function of darkon mass once m_h is specified. We show in Fig. 2(a) our results for $\sigma_{\rm el}$ in the SM3+D, with the choices of darkon and Higgs masses being the same as those in Fig. 1. To demonstrate the impact of the fourth generation, we display in Fig. 2(b) the ratio of $\sigma_{\rm el}$ in the SM4+D with $m_{t'} = 500$ GeV to $\sigma_{\rm el}$ in the SM3+D. The ratio curves for the SM4+D cases with $m_{t'} = 400$ and 600 GeV are similar to the one displayed. This figure indicates that at most of the m_D values considered the $\sigma_{\rm el}$ curves in the SM4+D for the three different Higgs masses are higher than the corresponding ones in the SM3+D. This increase ranges from a few percent to roughly 50% and comes from the $g_{NNh}^{\rm SM4}$ enhancement relative to $g_{NNh}^{\rm SM3}$ overcoming the $\lambda_{\rm SM4+D}$ suppression relative to $\lambda_{\rm SM3+D}$ mentioned in the preceding

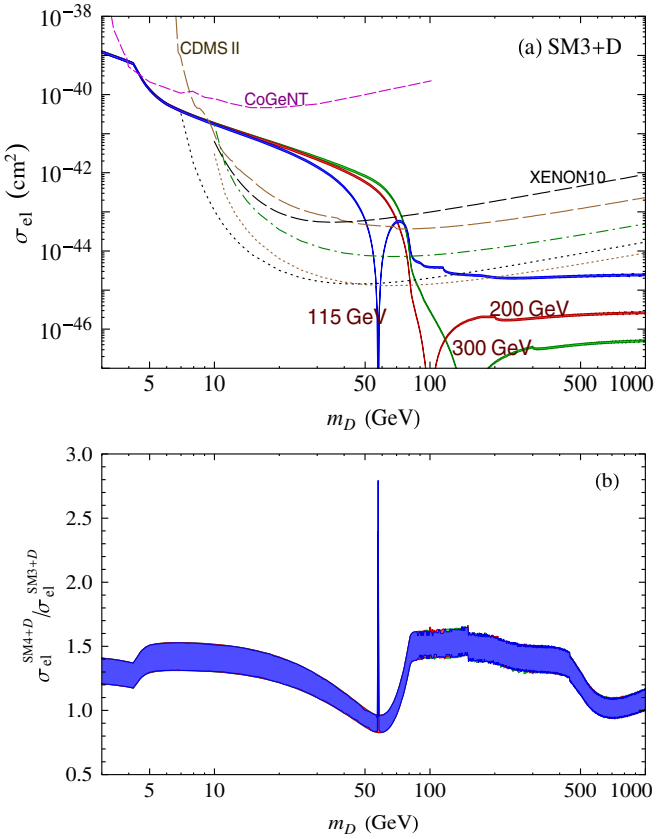

FIG. 2 (color online). (a) Darkon-nucleon elastic cross section $\sigma_{\rm el}$ as a function of darkon mass m_D for Higgs-mass values $m_h = 115$, 200, 300 GeV in SM3+D, compared to 90% C.L. upper limits from XENON10 (black dashed-curve), CDMS-II (brown [gray] dashed-curve), and CoGeNT (purple dashed-curve), as well as projected sensitivities of SuperCDMS at Soudan (green dot-dashed curve), SuperCDMS at Snolab (brown [gray] dotted curve), and XENON100 (black dotted curve). (b) Ratio of corresponding $\sigma_{\rm el}$ in SM4+D, with $m_{t'} = 500$ GeV, to $\sigma_{\rm el}$ in SM3+D.

section. The spike in Fig. 2(b) corresponds to that in Fig. 1(b) and hence belongs to the $m_h = 115$ GeV case.

In Fig. 2(a), we also plot the 90% C.L. upper-limit curves for the WIMP-nucleon spin-independent elastic cross section reported by the XENON10 [30], CDMS-II [32], and CoGeNT [33] experiments, along with the expected sensitivities of a number of future experiments [40]. For $m_D \lesssim 10$ GeV, there are also limits from CRESST-I [29] and TEXONO [31], but they are both above the predictions of the two models.

Comparing the prediction curves of both models to the experimental upper-bounds in Fig. 2, one can see that some portions of the darkon mass regions considered are excluded, but the greater part of them are still viable. More precisely, for $m_h = 115$, 200, and 300 GeV the XENON10 and CDMS-II limits have ruled out darkon masses from $\sim$9 GeV to between 70 and 80 GeV, except for the 50 GeV $< m_D <$ 70 GeV range in the $m_h = 115$ GeV case. Moreover, in the low-m_D sections of the plots the exclusion limit from CoGeNT can be seen to rule out part of the 4 GeV $\lesssim m_D \lesssim$ 5 GeV range. In contrast, darkon masses larger than 80 GeV or so are not yet probed by the current data from direct searches. As the projected sensitivities of future experiments in this figure suggest, SuperCDMS at Snolab and XENON100 may probe these models further to $m_D \sim 400$ GeV, but SuperCDMS at Soudan may be unlikely to provide much stronger constraints on the models than the present bounds.

It is interesting to point out that these two darkon models can accommodate the possibility that the excess events observed by CoGeNT originate from interactions with a relatively light WIMP of mass between 7 and 11 GeV [33], which is compatible with the two signal-like events detected by CDMS-II [32] if they are also interpreted as evidence for WIMP interactions. As one can infer from Fig. 2, for m_D values within this range the curves for the predicted $\sigma_{\rm el}$ each have some overlap with the possible signal region reported by CoGeNT [33]. This is more so if we take into account the uncertainties in g_{NNh} noted above, which could imply an increase in the predicted $\sigma_{\rm el}$ by up to a factor of 3.

Before moving on, it is worth remarking that, as Fig. 2 indicates, $\sigma_{\rm el}$ for a fixed m_h approaches a constant value as m_D becomes much greater than $m_{W,Z,h,t'}$. The reason is that in this large-m_D limit the ratio λ^2/m_D^2 is, as pointed out in the preceding section, approximately constant and $\sigma_{\rm el}$ in Eq. (5) is proportional to the same ratio, λ^2/m_D^2. Another observation from this figure is that the asymptotic value of $\sigma_{\rm el}$ decreases as m_h increases, which is in accord with Eq. (5). Hence, direct DM searches in the future may lack the sensitivity to probe the larger darkon masses if the Higgs mass is also large.

IV. SOME IMPLICATIONS FOR HIGGS SEARCHES AT COLLIDERS

Since the darkon sectors of the SM3+D and SM4+D both have only a small number of free parameters, the relevant ones here being λ, m_D, and m_h, it is possible to draw strong correlations among them [10]. This implies that these darkon models have a high degree of predictivity and that it is relatively simple to examine them, which would not require many different observables. We now consider this further by evaluating the Higgs decay into a pair of darkons, $h \to DD$, and discussing some of the implications for probing the darkon properties and for studying the Higgs boson at colliders, in light of the bounds obtained above from comparing with DM direct-detection data.

Using the λ values found in Sec. II, we compute the rate and branching ratio of $h \to DD$, which is an invisible mode due to the darkon being stable. The numbers we get are depicted in Fig. 3, where the Higgs and darkon mass choices are the same as those in Fig. 1. The SM3+D

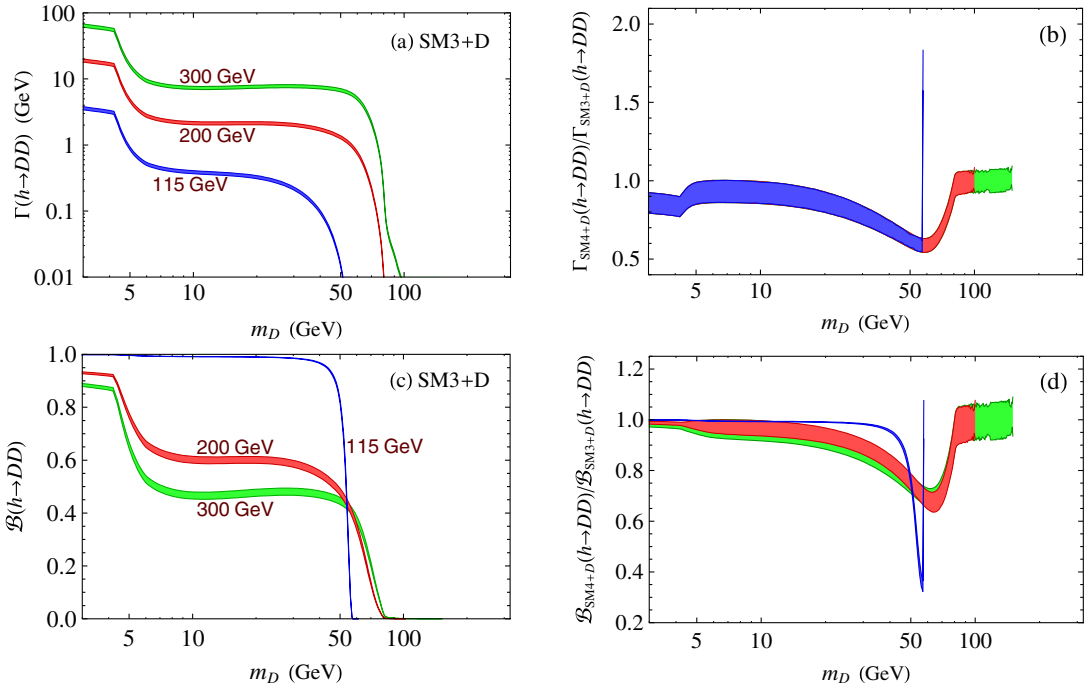

FIG. 3 (color online). (a,c) Partial width and branching ratio of invisible decay $h \to DD$ as functions of darkon mass m_D for Higgs-mass values $m_h = 115$, 200, 300 GeV in SM3+D. (b,d) Ratios of corresponding $\Gamma(h \to DD)$ and $\mathcal{B}(h \to DD)$ in SM4+D, with $m_{t'} = 500$ GeV, to their counterparts in SM3+D.

results are graphed in Figs. 3(a) and 3(c), whereas the impact of the fourth generation can be viewed in the ratio plots of Figs. 3(b) and 3(d), which compare the numbers in the two models. Since $\Gamma(h \to DD)$ is directly proportional to $|\lambda|^2$, the width ratio in Fig. 3(b) is none other than $\lambda^2_{\mathrm{SM4+D}}/\lambda^2_{\mathrm{SM3+D}}$ in the kinematically allowed region, $m_D \leq m_h/2$. The spikes in Figs. 3(b) and 3(d) again correspond to that in Fig. 1(b) and hence belong to the $m_h = 115$ GeV curves. Although the $h \to DD$ rate and branching ratio for $m_h = 115$ GeV vanish at the kinematical limit $m_D = 57.5$ GeV, the plots in Figs. 3(b) and 3(d) reflect the fact that the spike in Fig. 1(b) starts to appear slightly before this limit.

One can observe in Fig. 3 that the situations in the SM3+D and SM4+D are roughly similar when it comes to the effect of the additional process $h \to DD$ on the Higgs width if m_D not large, namely, that the sizable values of λ in Fig. 1 translate into huge enhancement of the Higgs width via $h \to DD$ and, consequently, an invisible branching ratio that is large. This is especially so if $2m_D < m_h < 2m_W$, in which case the Higgs partial width into standard particles is small. Although the fourth-generation quarks can cause the decay mode into a gluon pair, $h \to gg$, to dominate if $m_h \lesssim 140$ GeV [15], the inclusion of the darkon in the SM4+D leads to the dominance of $h \to DD$ instead.

A substantial Higgs invisible decay can be advantageous for testing the darkon models if the information gained from direct searches for DM is combined with that from the study of the Higgs boson at colliders. As found above, the greater part of the darkon mass range from about 9 to 80 GeV in the SM3+D and SM4+D have been ruled out by direct-detection data if the Higgs mass $m_h = 115$, 200, or 300 GeV, the main exception being the neighborhood of $m_D \sim 57.5$ GeV in the $m_h = 115$ GeV case. Since Fig. 3 shows that a Higgs boson with one of these masses decays dominantly or significantly into a darkon pair if $m_D \lesssim 50$ GeV, then the observation of such a Higgs boson with a sizable invisible branching-ratio might hint at inconsistencies of the models. An additional advantage of the potential enhancement of $h \to DD$ is that it can help lift some possible ambiguities in fixing the darkon mass from direct DM searches. As Fig. 2 indicates, for a given value of σ_{el} with m_h fixed there can be more than one value of m_D. Some of these discrete ambiguities may be resolved if the Higgs is discovered at a collider and its invisible branching ratio can be measured with sufficient precision [10]. All this illustrates that the interplay between DM direct searches and Higgs studies at colliders can yield crucial information about the darkon properties.

Another important implication of the possible dominance of $h \to DD$ is that it can alleviate some of the restrictions on Higgs masses in the SM4. For instance, at hadron colliders the prominent channel $gg \to h \to WW \to \ell\nu\ell\nu$ is expected to be enhanced in the SM4 due to the new quarks by up to a factor of 9 for 100 GeV $\lesssim m_h \lesssim$ 200 GeV, the measurement of which would also provide indirect evidence for the new quarks [13]. Preliminary

searches at the Tevatron for this channel have so far come back negative [13,24], thus excluding a large portion of this m_h range in the SM4. In the SM4+D, however, a dominant $h \to DD$ mode implies that the enhancement of $gg \to h \to WW \to \ell\nu\ell\nu$ would be reduced or even negated completely, and so the Higgs-mass constraints could be weakened or evaded.

An enhanced $\mathcal{B}(h \to DD)$ affects not only collider searches for the Higgs boson, but also decays which are mediated by or produce it. In the following two sections, we deal with such processes arising from the Higgs flavor-changing neutral couplings to quarks.

V. CONSTRAINTS FROM $B \to KDD$ DECAYS

As seen in Sec. III, direct DM searches with underground detectors currently being done or to be done in the near future are not expected to be sensitive to darkon masses below a few GeV. It turns out that such darkon masses can be probed using the decays of mesons containing the b quark. In this section we explore constraints available from the B-meson decay $B \to KDD$, which contributes to the B decay into K plus missing energy, $B \to K\not{E}$. One could carry out a similar analysis using $B \to K^*DD$, but we will not do so here. We will also briefly comment on the spin-one bottomonium decay $\Upsilon \to DD\gamma$.

Since the Higgs boson h is the only SM particle to which D couples, $B \to KDD$ is induced by the flavor-changing b-quark decay $b \to sh^* \to sDD$, where the effective bsh coupling is generated by loop diagrams containing up-type quarks and the W boson. These transitions have been dealt with previously in the context of the SM3+D in Refs. [7,12]. Generalizing some of the formulas given therein to the SM4+D, we can express the effective Hamiltonian for $b \to sh^* \to sDD$ as

$$\mathcal{H}_{b\to sDD} = \frac{\lambda g_{bs} m_b}{2m_h^2}\bar{s}(1+\gamma_5)bD^2, \tag{8}$$

where

$$g_{bs} = \frac{3g^2}{64\pi^2}(\lambda_t^{bs} x_t + \lambda_{t'}^{bs} x_{t'}), \quad x_q = \frac{m_q^2}{m_W^2}, \quad \lambda_q^{bs} = V_{qs}^* V_{qb}, \tag{9}$$

with V_{kl} being the elements of the 4×4 Cabibbo-Kobayashi-Maskawa (CKM4) matrix, and contributions from u and c quarks have been neglected. Hence the SM3 + D expression for g_{bs} does not contain the $\lambda_{t'}^{bs} x_{t'}$ term.

The amplitude for $B^- \to K^- DD$ is then

$$\mathcal{M}(B^- \to K^- DD) = \frac{\lambda g_{bs} m_B^2}{m_h^2} f_0(\hat{s}), \tag{10}$$

where $f_0(\hat{s}) = 0.3\exp(0.63\hat{s}/m_B^2 - 0.095\hat{s}^2/m_B^4 + 0.591\hat{s}^3/m_B^6)$ is the relevant $B \to K$ form-factor [7], with $\hat{s} = (p_B - p_K)^2$, and the approximation $(m_B^2 - m_K^2)/(m_b - m_s) \simeq m_B^2/m_b$ has been made. It follows that

$$\Gamma(B^+ \to K^+ DD) = \frac{\lambda^2}{m_h^4}\frac{|g_{bs}|^2 m_B}{512\pi^3} I(m_D), \tag{11}$$

where a factor of $1/2$ has been included to account for the identical D's in the final state and

$$I(m_D) = \int_{4m_D^2}^{(m_B-m_K)^2} d\hat{s}(f_0(\hat{s}))^2 \times \sqrt{1-\frac{4m_D^2}{\hat{s}}}\sqrt{(m_B^2 - m_K^2 - \hat{s})^2 - 4m_K^2\hat{s}}. \tag{12}$$

We note that our formula for the $B \to KDD$ rate agrees with the corresponding one obtained in Ref. [12], but is 4 times smaller than that given in Ref. [7].[2] Since for $m_D \ll m_h$ we can simplify Eq. (4) to

$$\sigma_{\rm ann} v_{\rm rel} \simeq \frac{\lambda^2}{m_h^4}\frac{4v^2\sum_i \Gamma(\tilde{h} \to X_i)}{m_D}, \tag{13}$$

we can rewrite Eq. (11) as

$$\Gamma(B^+ \to K^+ DD) \simeq \frac{|g_{bs}|^2 m_B I(m_D)}{2048\pi^3 v^2}\frac{(\sigma_{\rm ann} v_{\rm rel}) m_D}{\sum_i \Gamma(\tilde{h} \to X_i)}, \tag{14}$$

where both $\sigma_{\rm ann} v_{\rm rel}$ and $\Sigma_i \Gamma(\tilde{h} \to X_i)$ have m_D dependence. We can get constraints on the parameter space $m_D \le (m_B - m_K)/2$ by comparing this prediction with the experimental information on the B decay into a kaon plus missing energy, which receives contributions from $B \to KDD$ and $B \to K\nu\bar{\nu}$. We first update the constraints in the SM3+D and then discuss the SM4+D case.

The branching ratio $\mathcal{B}(B \to KDD)$ evaluated in the SM3+D using Eq. (14), with the $\lambda_{t'}^{bs} x_{t'}$ term in g_{bs} dropped, involves large uncertainties which come mainly from the calculation of the total width $\Sigma_i \Gamma(\tilde{h} \to X_i)$ for $m_{\tilde{h}}$ under a few GeV. In the case of the physical h, for $m_h \lesssim 2$ GeV the theoretical rate of the important channel $h \to$ hadrons is well known to contain significant uncertainties [41,42]. In estimating the $\tilde{h}$ total width, for $2m_\pi \le m_{\tilde{h}} \le 1.4$ GeV we adopt the $\Gamma(h \to \text{hadrons})$ results from Ref. [42], whereas for smaller and larger values of $m_{\tilde{h}}$ we simply use the perturbative formulas for Higgs decays [43]. We graph the numerical $\mathcal{B}(B \to KDD)$ as a function of m_D in Fig. 4, which is to be compared with experimental data.

The latest search for the decay $B^+ \to K^+\nu\bar{\nu}$ has produced the branching-ratio limit $\mathcal{B}_{\rm exp}(B^+ \to K^+\nu\bar{\nu}) < 14\times 10^{-6}$ [44]. On the theoretical side, the most recent calculations in the SM3 yield $\mathcal{B}(B^+ \to K^+\nu\bar{\nu})$ numbers between 3.6×10^{-6} and 5.1×10^{-6}, with errors of order

[2] This can be traced to a factor of $1/2$ apparently missing in the expression for the $B \to KDD$ amplitude in the Eq. (6) of the first paper in Ref. [7].

15% [45]. Accordingly, it is reasonable to take $\mathcal{B}_{\rm exp}(B^+ \to K^+ \not{E}) \simeq \mathcal{B}_{\rm exp}(B^+ \to K^+ \nu\bar{\nu})$, from which we can subtract the SM3 value of $\mathcal{B}(B^+ \to K^+ \nu\bar{\nu})$ in order to require that $\mathcal{B}(B^+ \to K^+ DD) < 1 \times 10^{-5}$ in the SM3+D.

We can see from Fig. 4 that $\mathcal{B}_{\rm SM3+D}(B^+ \to K^+ DD) > 1 \times 10^{-5}$ for $m_D \lesssim 1.5$ GeV. Recalling the hadronic uncertainties mentioned above, we can then conclude that in the SM3+D much of this range of m_D values, especially $m_D \lesssim 0.4$ GeV, is excluded by the data. We would need improved data from future measurements of $B \to K \not{E}$ before we could disallow more darkon masses within the $m_D < 2.4$ GeV region. These conclusions are similar to those made in Ref. [7] due partly to the stronger experimental limit at present and partly to the overestimate of their $\mathcal{B}(B \to KDD)$.

In the SM4+D, the prediction for $\Gamma(B \to KDD)$ is modified due to the presence of the new quarks, t' and b'. The loop-induced effective coupling g_{bs} in Eq. (14) receives a t'-quark contribution as given in Eq. (9). To examine its effect on $\Gamma(B \to KDD)$, we need to compare $g_{bs}^{\rm SM4}$ to $g_{bs}^{\rm SM3}$. For concreteness, we take the relevant CKM4 elements extracted in Ref. [19] from a global fit for the SM4. Accordingly, we can expect that the numbers we use are typical values for the model. Thus, with $\lambda_t^{bs} = 0.04$ in $g_{bs}^{\rm SM3}$, we find $|g_{bs}^{\rm SM4}/g_{bs}^{\rm SM3}|^2$ for $m_{t'} = 400$ and 500 GeV to be similar in value, $\sim$1.2, but it goes up to 1.6 for $m_{t'} = 600$ GeV. In addition, the presence of t' and b' affects the total width $\Sigma_i \Gamma(\tilde{h} \to X_i)$ in Eq. (14) mainly via their contributions to $\tilde{h} \to$ hadrons due to the quark-loop induced $\tilde{h} \to gg$, as already mentioned earlier. Despite the hadronic uncertainties, this implies that the enhancement of the $\tilde{h}$ total width in the SM4 compared to the SM3 can be expected to be less than $(5/3)^2 \simeq 2.8$ if $2m_\pi \le m_{\tilde{h}} \le 2m_c$, where 5 and 3 are the numbers of heavy quarks in the two models, respectively, for this $m_{\tilde{h}}$ range. This enhancement decreases to no more than 25% after the $\tilde{h} \to c\bar{c}$ channel is open. We can then conclude that the effects of these two factors on $\Gamma(B \to KDD)$ in the SM4+D amount to changes to the rate in the SM3+D by no more than a factor of 2 in either direction, implying that the curve in Fig. 4 would not be very different in the SM4+D. Since the prediction for $\mathcal{B}(B^+ \to K^+ \nu\bar{\nu})$ is raised by at most 20% in the SM4 [18], the empirical bound on $\mathcal{B}(B \to KDD)$ in the SM4+D can be taken to be unchanged compared to that in the SM3+D. It follows that the constraints on the darkon masses within the $m_D < 2.4$ GeV range in the SM4+D are similar to those in the SM3+D.

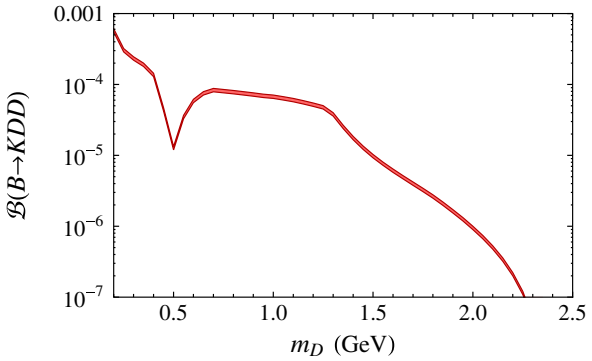

FIG. 4 (color online). Branching ratio of $B^+ \to K^+ DD$ as a function of darkon mass m_D in SM3+D.

We should also mention that for $m_D \lesssim 170$ MeV an additional restriction is provided by the kaon decay $K^+ \to \pi^+ \not{E}$, which receives a contribution from $K^+ \to \pi^+ DD$. The agreement between the SM3 expectation and experimental data on $K^+ \to \pi^+ \not{E}$ implies that for $m_D \lesssim 170$ MeV the SM3+D is already ruled out [7], as is the SM4+D. This is consistent with what can be inferred from the low-m_D end of Fig. 4.

For the larger range $m_D \lesssim 5$ GeV, there may also be constraints available from future measurements of the decays $\Upsilon \to DD\gamma$. Presently, the existing experimental limits for $\Upsilon \to \gamma +$ invisible are not yet strong enough to impose restrictions on these darkon models [11].

VI. FCNC DECAYS $Q \to qDD$

The presence of the new quarks in the SM4+D can have important implications for probing the darkon sector that are lacking or absent in the SM3+D. In the SM3 the flavor-changing neutral current (FCNC) top-quark decay $t \to ch$ is known to be very suppressed, with a branching ratio estimated to be between 10^{-15} and 10^{-13} [46,47], but in the SM4 the branching ratio can be enhanced by several orders of magnitude [19,48]. We expect that in the SM4+D the related decay $t \to ch^* \to cDD$, if kinematically allowed, can be similarly enhanced. These processes could be detectable at the LHC after its operation reaches full capacity in the near future. The LHC, and perhaps the Tevatron, may also be able to produce the new quarks, t' and b', if they exist, in a similar way as the colliders can produce the t quark, albeit fewer of them due to their bigger masses. It is therefore of interest as well to explore their FCNC decays involving the darkon, $t' \to (c, t)h^* \to (c, t)DD$ and $b' \to (s, b)h^* \to (s, b)DD$, which may have observable rates. These decays could, in principle, probe darkon masses from zero all the way up to half the mass difference between the initial and final quarks, $(m_Q - m_q)/2$, hence covering potentially wider m_D ranges than those covered by some of the DM direct searches in the future. Here we estimate the branching ratios of these FCNC decays involving the darkon. The related decays with the u and d quarks, $t^{(\prime)} \to uDD$ and $b' \to dDD$, are comparatively suppressed due to the less favorable CKM4 factors.

The Lagrangian describing the FCNC transition $Q \to qh$ involving a heavy quark Q and a lighter quark q can be written as

$$\mathcal{L}_{Qqh} = \bar{q}(g_{\rm L}^{Qq} P_{\rm L} + g_{\rm R}^{Qq} P_{\rm R}) Q h, \tag{15}$$

where $P_{\rm L,R} = \frac{1}{2}(1 \mp \gamma_5)$ and the loop-induced couplings

$g^{Qq}_{\mathrm{L,R}}$ generally depend not only on the internal quark (and W) masses and the CKM matrix elements, but also on the masses and momenta of the external particles. The amplitude for $Q \to qh^* \to qDD$ is then

$$\mathcal{M}(Q \to qDD) = \frac{2\lambda v \bar{q}(g^{Qq}_{\mathrm{L}} P_{\mathrm{L}} + g^{Qq}_{\mathrm{R}} P_{\mathrm{R}})Q}{m_h^2 - \bar{s} - i\Gamma_h m_h}, \tag{16}$$

where $\bar{s} = (p_Q - p_q)^2$. This yields the decay rate

$$\Gamma(Q \to qDD) = \frac{\lambda^2 v^2}{256\pi^3 m_Q^3} \int_{4m_D^2}^{(m_Q - m_q)^2} d\bar{s} \sqrt{1 - \frac{4m_D^2}{\bar{s}}} \sqrt{(m_Q^2 - m_q^2 - \bar{s})^2 - 4m_q^2 \bar{s}} \times \frac{(|g^{Qq}_{\mathrm{L}}|^2 + |g^{Qq}_{\mathrm{R}}|^2)(m_Q^2 + m_q^2 - \bar{s}) + 4\,\mathrm{Re}(g^{Qq*}_{\mathrm{L}} g^{Qq}_{\mathrm{R}}) m_Q m_q}{(\bar{s} - m_h^2)^2 + \Gamma_h^2 m_h^2}. \tag{17}$$

For $2m_D < m_h < m_Q - m_q$, the Higgs-pole contribution dominates this integral, and so one has $\Gamma(Q \to qDD) \simeq \Gamma(Q \to qh)\mathcal{B}(h \to DD)$.

The effective couplings $g^{Qq}_{\mathrm{L,R}}$ in the SM have been evaluated previously for arbitrary values of the external and internal masses [48–50]. We make use of the formulas provided in Ref. [50]. In our numerical illustration below, we take $m_h = 115$ GeV and $m_{t'} = 500$ GeV, as well as the pertinent elements of the CKM4 matrix extracted from a global fit in Ref. [19]. To determine the branching ratios, we normalize the decay rates according to

$$\mathcal{B}(t \to cDD) = \frac{\Gamma(t \to cDD)}{\Gamma(t \to bW)}, \tag{18}$$

$$\mathcal{B}(t' \to qDD) = \frac{\Gamma(t' \to qDD)}{\Gamma(t' \to bW) + \Gamma(t' \to sW)}, \tag{19}$$

$$\mathcal{B}(b' \to qDD) = \frac{\Gamma(b' \to qDD)}{\Gamma(b' \to tW) + \Gamma(b' \to cW)}, \tag{20}$$

following Ref. [19] in the $Q \to qh$ cases. We display the results in Fig. 5.

Estimates suggest that $t \to ch$ can be detected at the LHC if its branching ratio is several times 10^{-5} or higher [47]. In the presence of the darkon, if $h \to DD$ is leading, $t \to ch \to cDD$ is more likely to occur than other $t \to ch \to cX$ modes. In that case, however, as Fig. 5 indicates, $\mathcal{B}(t \to cDD) \lesssim 1.0 \times 10^{-8}$ and as a consequence $t \to cDD$ probably will not be observable in the near future. The branching ratio could be several times higher if $m_{t'} \sim 700$ GeV, but this already exceeds the perturbative unitarity upper-bound $m_{t'} \sim 550$ GeV [13,27].

In contrast, the t' and b' numbers in Fig. 5 are much greater: $\mathcal{B}(t' \to cDD) \lesssim 8.2 \times 10^{-5}$, $\mathcal{B}(t' \to tDD) \lesssim 1.4 \times 10^{-3}$, $\mathcal{B}(b' \to sDD) \lesssim 3.1 \times 10^{-4}$, and $\mathcal{B}(b' \to bDD) \lesssim 3.3 \times 10^{-3}$. Since $t' \to qh$ and $b' \to qh$ decays with branching ratios between 10^{-4} and 10^{-2} are expected to be within the reach of the LHC [19,48], we may expect that these $t' \to qDD$ and $b' \to qDD$ decays would also be detectable at the LHC despite their final states involving missing energy. Once they are measured, comparing the results with those from DM direct searches could provide additional consistency tests for the darkon models.

VII. CONCLUSIONS

We have explored one of the simplest dark-matter models, the SM4+D, consisting of the standard model with four generations and a real gauge-singlet scalar, the dar-

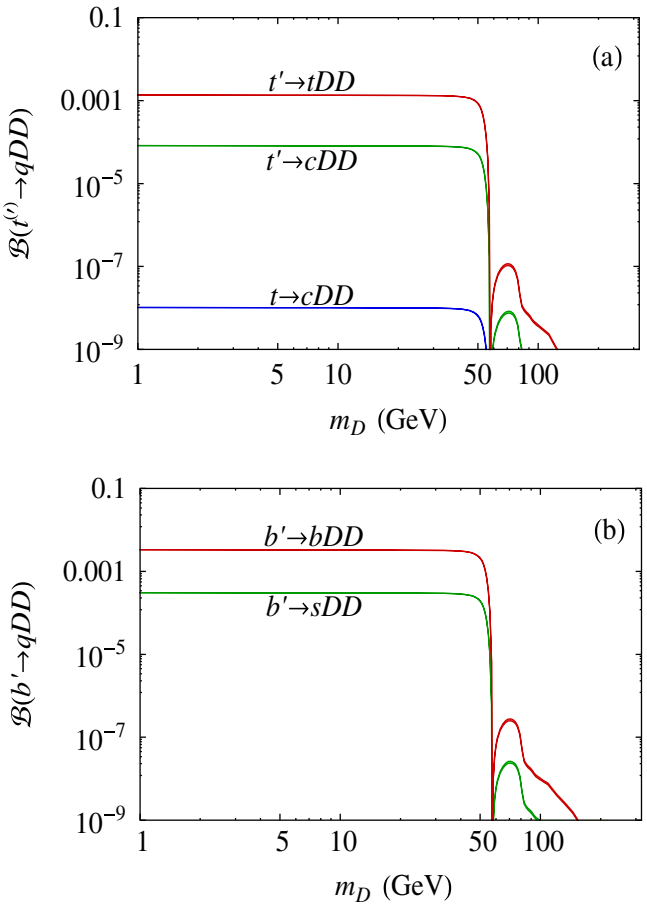

FIG. 5 (color online). Branching ratios of (a) $t \to cDD$, $t' \to cDD$, and $t' \to tDD$ and (b) $b' \to sDD$ and $b' \to bDD$ as functions of darkon mass m_D for Higgs mass $m_h = 115$ GeV in SM4+D with $m_{t'} = 500$ GeV.

kon, to play the role of WIMP dark matter. This model possesses not only the phenomenologically interesting features of the SM4, but also a high degree of predictivity in its DM sector. We have investigated constraints on the SM4+D from DM direct-search experiments and from B-meson decay into a kaon plus missing energy. Compared to the SM3+D case, the resulting bounds in the SM4+D are similar, namely, that for the representative Higgs masses chosen most of the darkon masses between roughly 4 to 80 GeV are excluded by the direct searches and that much of the mass region below 1.5 GeV is also excluded by the B decay data. Interestingly, the SM4+D as well as the SM3+D can also accommodate the possible interpretation that the excess events recently measured by the CDMS-II and CoGeNT experiments were due to interactions with a light WIMP of mass around 9 GeV. Darkon masses greater than 80 GeV in the two models are still viable and can be probed by future direct searches.

We have discussed the complementarity of DM direct searches and Higgs studies at colliders in testing the darkon sector of the SM4+D. This can be crucial for a relatively light Higgs boson, which may decay substantially into the invisible darkons. Accordingly, we have pointed out that existence of the darkon could lead to the weakening or evasion of some of the restrictions on the Higgs mass in the presence of fourth-generation fermions.

We have considered some implications of the SM4+D that are lacking or absent in the SM3+D as far as probing the darkon properties is concerned. In particular, we have examined the Higgs-mediated FCNC decays $t \to cDD$, $t' \to (c, t)DD$, and $b' \to (s, b)DD$, which may have observable rates at current or future colliders. These processes promptly proceed from the $Q \to qh$ transitions if the decay mode $h \to DD$ is dominant. Although the $t \to cDD$ branching-ratio is enhanced by several orders of magnitude compared to that in the SM3+D, reaching the 10^{-8} level, this decay is still unlikely to be measurable in the near future. In contrast, the branching ratios of $t' \to qDD$ and $b' \to qDD$ can be as large as a few times 10^{-3}, which may be detectable at the LHC. If observed, they would offer extra means to test the models, covering darkon masses from zero up to hundreds of GeV.

ACKNOWLEDGMENTS

This work was partially supported by NSC and NCTS.

[1] C. Amsler *et al.* (Particle Data Group), Phys. Lett. B **667**, 1 (2008).
[2] V. Silveira and A. Zee, Phys. Lett. **161B**, 136 (1985).
[3] J. McDonald, Phys. Rev. D **50**, 3637 (1994).
[4] C. P. Burgess, M. Pospelov, and T. ter Veldhuis, Nucl. Phys. **B619**, 709 (2001).
[5] M. C. Bento, O. Bertolami, R. Rosenfeld, and L. Teodoro, Phys. Rev. D **62**, 041302 (2000); M. C. Bento, O. Bertolami, and R. Rosenfeld, Phys. Lett. B **518**, 276 (2001); D. E. Holz and A. Zee, Phys. Lett. B **517**, 239 (2001); J. McDonald, Phys. Rev. Lett. **88**, 091304 (2002); H. Davoudiasl, R. Kitano, T. Li, and H. Murayama, Phys. Lett. B **609**, 117 (2005); S. h. Zhu, Chin. Phys. Lett. **24**, 381 2007; X. G. He, T. Li, X. Q. Li, and H. C. Tsai, Mod. Phys. Lett. A **22**, 2121 (2007); S. Andreas, T. Hambye, and M. H. G. Tytgat, J. Cosmol. Astropart. Phys. 10 (2008) 034; C. E. Yaguna, J. Cosmol. Astropart. Phys. 03 (2009) 003; S. M. Carroll, S. Mantry, and M. J. Ramsey-Musolf, Phys. Rev. D **81**, 063507 (2010); T. E. Clark, B. Liu, S. T. Love, and T. ter Veldhuis, Phys. Rev. D **80**, 075019 (2009); R. N. Lerner and J. McDonald, Phys. Rev. D **80**, 123507 (2009); M. Gonderinger, Y. Li, H. Patel, and M. J. Ramsey-Musolf, J. High Energy Phys. 01 (2010) 53; S. Mantry, AIP Conf. Proc. **1241**, 1025 (2010); M. Kadastik, K. Kannike, A. Racioppi, and M. Raidal, arXiv:0912.3797; M. Farina, D. Pappadopulo, and A. Strumia, Phys. Lett. B **688**, 329 (2010); M. Aoki, S. Kanemura, and O. Seto, Phys. Lett. B **685**, 313 (2010); M. Asano and R. Kitano, Phys. Rev. D **81**, 054506 (2010); S. Andreas, C. Arina, T. Hambye, F. S. Ling, and M. H. G. Tytgat, arXiv:1003.2595.
[6] G. Cynolter, E. Lendvai, and G. Pocsik, Acta Phys. Pol. B **36**, 827 (2005).
[7] C. Bird, P. Jackson, R. Kowalewski, and M. Pospelov, Phys. Rev. Lett. **93**, 201803 (2004); C. Bird, R. Kowalewski, and M. Pospelov, Mod. Phys. Lett. A **21**, 457 (2006).
[8] V. Barger, P. Langacker, M. McCaskey, M. J. Ramsey-Musolf, and G. Shaughnessy, Phys. Rev. D **77**, 035005 (2008).
[9] X. G. He, T. Li, X. Q. Li, J. Tandean, and H. C. Tsai, Phys. Rev. D **79**, 023521 (2009).
[10] X. G. He, T. Li, X. Q. Li, J. Tandean, and H. C. Tsai, Phys. Lett. B **688**, 332 (2010)
[11] G. K. Yeghiyan, Phys. Rev. D **80**, 115019 (2009); arXiv:0910.2071.
[12] C. S. Kim, S. C. Park, K. Wang, and G. Zhu, Phys. Rev. D **81**, 054004 (2010).
[13] B. Holdom, W. S. Hou, T. Hurth, M. L. Mangano, S. Sultansoy, and G. Unel, PMC Phys. A **3**, 4 (2009).
[14] M. Maltoni, V. A. Novikov, L. B. Okun, A. N. Rozanov, and M. I. Vysotsky, Phys. Lett. B **476**, 107 (2000); H. J. He, N. Polonsky, and S. f. Su, Phys. Rev. D **64**, 053004 (2001); J. Alwall *et al.*, Eur. Phys. J. C **49**, 791 (2007); V. A. Novikov, A. N. Rozanov, and M. I. Vysotsky, Phys. At. Nucl. **73**, 636 (2010).
[15] G. D. Kribs, T. Plehn, M. Spannowsky, and T. M. P. Tait, Phys. Rev. D **76**, 075016 (2007).

[16] M. S. Chanowitz, Phys. Rev. D **79**, 113008 (2009); J. Erler and P. Langacker, Phys. Rev. Lett. **105**, 031801 (2010).

[17] M. Bobrowski, A. Lenz, J. Riedl, and J. Rohrwild, Phys. Rev. D **79**, 113006 (2009); A. J. Buras *et al.*, arXiv:1002.2126.

[18] A. Soni, A. K. Alok, A. Giri, R. Mohanta, and S. Nandi, Phys. Lett. B **683**, 302 (2010); Phys. Rev. D **82**, 033009 (2010)

[19] G. Eilam, B. Melic, and J. Trampetic, Phys. Rev. D **80**, 116003 (2009).

[20] A. Arhrib and W. S. Hou, Eur. Phys. J. C **27**, 555 (2003); Phys. Rev. D **80**, 076005 (2009); W. S. Hou, M. Nagashima, and A. Soddu, Phys. Rev. D **72**, 115007 (2005); **76**, 016004 (2007); W. S. Hou, M. Nagashima, G. Raz, and A. Soddu, J. High Energy Phys. 09 (2006) 012; W. S. Hou, H. n. Li, S. Mishima, and M. Nagashima, Phys. Rev. Lett. **98**, 131801 (2007); J. A. Herrera, R. H. Benavides, and W. A. Ponce, Phys. Rev. D **78**, 073008 (2008); W. S. Hou and C. Y. Ma, Phys. Rev. D **82**, 036002 (2010).

[21] W. S. Hou, Chin. J. Phys. (Taipei) **47**, 134 (2009); R. Fok and G. D. Kribs, Phys. Rev. D **78**, 075023 (2008); Y. Kikukawa, M. Kohda, and J. Yasuda, Prog. Theor. Phys. **122**, 401 (2009).

[22] P. H. Frampton, P. Q. Hung, and M. Sher, Phys. Rep. **330**, 263 (2000); T. Yanir, J. High Energy Phys. 06 (2002) 044; K. Belotsky, D. Fargion, M. Khlopov, R. Konoplich, and K. Shibaev, Phys. Rev. D **68**, 054027 (2003); B. Holdom, J. High Energy Phys. 08 (2006) 076; 03 (2007) 063; 08 (2007) 069; Phys. Lett. B **686**, 146 (2010); G. Burdman and L. Da Rold, J. High Energy Phys. 12 (2007) 086; P. Q. Hung and M. Sher, Phys. Rev. D **77**, 037302 (2008); W. S. Hou, F. F. Lee, and C. Y. Ma, Phys. Rev. D **79**, 073002 (2009); G. Burdman, L. Da Rold, and R. D. Matheus, arXiv:0912.5219; O. Antipin, M. Heikinheimo, and K. Tuominen, J. High Energy Phys. 10 (2009) 018; J. High Energy Phys. 07 (2010) 52; M. T. Frandsen, I. Masina, and F. Sannino, Phys. Rev. D **81**, 035010 (2010); P. Q. Hung and C. Xiong, arXiv:0911.3890; arXiv:0911.3892; M. Hashimoto, Phys. Rev. D **81**, 075023 (2010); J. Alwall, J. L. Feng, J. Kumar, and S. Su, Phys. Rev. D **81**, 114027 (2010); W. S. Hou, Y. Y. Mao, and C. H. Shen, arXiv:1003.4361; W. S. Hou and F. F. Lee, arXiv:1004.2359; B. Holdom and Q. S. Yan, arXiv:1004.3031.

[23] X. G. He and S. Pakvasa, Phys. Lett. **156B**, 236 (1985); Nucl. Phys. **B278**, 905 (1986); K. S. Babu, X. G. He, X. Li, and S. Pakvasa, Phys. Lett. B **205**, 540 (1988); E. Golowich, J. Hewett, S. Pakvasa, and A. A. Petrov, Phys. Rev. D **76**, 095009 (2007); **79**, 114030 (2009).

[24] N. B. Schmidt, S. A. Cetin, S. Istin, and S. Sultansoy, Eur. Phys. J. C **66**, 119 (2010); E. Nagy, *Second Workshop on Beyond 3 Generation Standard Model, Taipei, Taiwan, 2010* (unpublished).

[25] E. W. Kolb and M. Turner, *The Early Universe* (Westview Press, Boulder, 1990).

[26] A. Lister (CDF Collaboration), arXiv:0810.3349; T. Aaltonen *et al.* (CDF Collaboration), Phys. Rev. Lett. **104**, 091801 (2010).

[27] M. S. Chanowitz, M. A. Furman, and I. Hinchliffe, Phys. Lett. B **78**, 285 (1978); Nucl. Phys. **B153**, 402 (1979).

[28] E. Komatsu *et al.*, arXiv:1001.4538.

[29] G. Angloher *et al.*, Astropart. Phys. **18**, 43 (2002).

[30] J. Angle *et al.* (XENON Collaboration), Phys. Rev. Lett. **100**, 021303 (2008); E. Aprile *et al.*, Phys. Rev. C **79**, 045807 (2009).

[31] S. T. Lin *et al.* (TEXONO Collaboration), Phys. Rev. D **79**, 061101 (2009).

[32] Z. Ahmed *et al.* (CDMS-II Collaboration), arXiv:0912.3592.

[33] C. E. Aalseth *et al.* (CoGeNT collaboration), arXiv:1002.4703.

[34] I. G. Irastorza, arXiv:0911.2855.

[35] For recent reviews, see W. de Boer, AIP Conf. Proc. **1078**, 108 (2008); **1200**, 165 (2010); X. G. He, Mod. Phys. Lett. A **24**, 2139 (2009).

[36] M. A. Shifman, A. I. Vainshtein, and V. I. Zakharov, Phys. Lett. **78B**, 443 (1978); S. Dawson and H. E. Haber, in *Proceedings of Workshop on High Energy Physics Phenomenology, Bombay, India, 1989*, edited by D. P. Roy and P. Roy (World Scientific, Singapore, 1989).

[37] T. P. Cheng, Phys. Rev. D **38**, 2869 (1988); H. Y. Cheng, Phys. Lett. B **219**, 347 (1989).

[38] J. Gasser, H. Leutwyler, and M. E. Sainio, Phys. Lett. B **253**, 252 (1991).

[39] J. R. Ellis, K. A. Olive, and C. Savage, Phys. Rev. D **77**, 065026 (2008); H. Ohki *et al.*, Phys. Rev. D **78**, 054502 (2008).

[40] R. Gaitskell, V. Mandic, and J. Filippini, http://dmtools.berkeley.edu/limitplots.

[41] S. Raby and G. B. West, Phys. Rev. D **38**, 3488 (1988); T. N. Truong and R. S. Willey, Phys. Rev. D **40**, 3635 (1989).

[42] J. F. Donoghue, J. Gasser, and H. Leutwyler, Nucl. Phys. **B343**, 341 (1990).

[43] A. Djouadi, Phys. Rep. **457**, 1 (2008).

[44] K. F. Chen *et al.* (BELLE Collaboration), Phys. Rev. Lett. **99**, 221802 (2007).

[45] W. Altmannshofer, A. J. Buras, D. M. Straub, and M. Wick, J. High Energy Phys. 04 (2009) 022; J. F. Kamenik and C. Smith, Phys. Lett. B **680**, 471 (2009); M. Bartsch, M. Beylich, G. Buchalla, and D. N. Gao, J. High Energy Phys. 11 (2009) 011.

[46] G. Eilam, J. L. Hewett, and A. Soni, Phys. Rev. D **44**, 1473 (1991); **59**, 039901(E) (1998); J. L. Hewett, T. Takeuchi, and S. D. Thomas, arXiv:hep-ph/9603391; B. Mele, S. Petrarca, and A. Soddu, Phys. Lett. B **435**, 401 (1998).

[47] J. A. Aguilar-Saavedra and G. C. Branco, Phys. Lett. B **495**, 347 (2000); J. A. Aguilar-Saavedra, Acta Phys. Pol. B **35**, 2695 (2004).

[48] A. Arhrib and W. S. Hou, J. High Energy Phys. 07 (2006) 009.

[49] P. Krawczyk, Z. Phys. C **44**, 509 (1989); W. S. Hou and R. G. Stuart, Phys. Rev. D **43**, 3669 (1991).

[50] G. Eilam, B. Haeri, and A. Soni, Phys. Rev. D **41**, 875 (1990).